

## Thermal noise in confined fluids

T. Sanghi and N. R. Aluru<sup>a)</sup>

*Department of Mechanical Science and Engineering, Beckman Institute for Advanced Science and Technology, University of Illinois at Urbana-Champaign, Urbana, Illinois 61801, USA*

(Received 15 May 2014; accepted 15 October 2014; published online 5 November 2014)

In this work, we discuss a combined memory function equation (MFE) and generalized Langevin equation (GLE) approach (referred to as MFE/GLE formulation) to characterize thermal noise in confined fluids. Our study reveals that for fluids confined inside nanoscale geometries, the correlation time and the time decay of the autocorrelation function of the thermal noise are not significantly different across the confinement. We show that it is the strong cross-correlation of the mean force with the molecular velocity that gives rise to the spatial anisotropy in the velocity-autocorrelation function of the confined fluids. Further, we use the MFE/GLE formulation to extract the thermal force a fluid molecule experiences in a MD simulation. Noise extraction from MD simulation suggests that the frequency distribution of the thermal force is non-Gaussian. Also, the frequency distribution of the thermal force near the confining surface is found to be different in the direction parallel and perpendicular to the confinement. We also use the formulation to compute the noise correlation time of water confined inside a (6,6) carbon-nanotube (CNT). It is observed that inside the (6,6) CNT, in which water arranges itself in a highly concerted single-file arrangement, the correlation time of thermal noise is about an order of magnitude higher than that of bulk water. © 2014 AIP Publishing LLC. [<http://dx.doi.org/10.1063/1.4900501>]

### I. INTRODUCTION

Thermal noise is the spontaneous microscopic fluctuations that occur naturally in a molecular system at finite temperature. With the advent of nanotechnology, there has been considerable interest in understanding the role of thermal fluctuations in nanofluidic dynamics and transport. It has been argued that thermal fluctuations can influence the flow characteristics and are expected to play a significant role in nanoscale transport.<sup>1,2</sup> An understanding of the interplay of thermal noise on the fluid dynamics and transport inside nanoscale systems is essential for understanding the mechanism of distinctive nanoscale phenomena such as single-file transport<sup>3</sup> and a possibility of thermal noise induced/assisted unidirectional transport.<sup>4</sup> In the last decade, few theoretical and molecular dynamics (MD) simulation studies have been performed that report the unforeseen role of thermal fluctuations in nanofluidic transport. Kalra, Garde, and Hummer<sup>3</sup> in their MD simulation of osmotic flow through a carbon-nanotube (CNT) report that the water flow is stochastic in nature and the flow rate is governed by thermal fluctuations. Detcherry and Bocquet<sup>5,6</sup> explored the impact of hydrodynamic fluid fluctuations on the transport of mass and charge in nanopores. Recently, Wan, Hu, and Fang<sup>4</sup> using a toy model showed that thermal noise may induce a biased (unidirectional) transport in a spatially asymmetric nanoscale dimension system, provided the correlation time of the thermal fluctuations is comparable to the characteristic time scale of the system. Though these studies highlight the relevance of thermal fluctuations in nanofluidic dynamics and transport, a general methodology that can be used to characterize and

understand thermal fluctuations in nanofluidic systems is, however, lacking.

Conventionally, equilibrium thermal fluctuations are modeled as “White” noise, which means that thermal fluctuations do not have any time scale associated with them and exist independently of the underlying physical process.<sup>7</sup> This assumption provides a reasonable description in systems where the correlation time of thermal noise is much smaller than the characteristic time scales of the system (see Ref. 8 for discussion on different time scales associated with molecular motion). However, in many fluidic systems, specifically for fluids confined inside nanometer scale geometries, the White noise assumption might be insufficient or invalid. In this work, we discuss a combined memory function equation (MFE) and generalized Langevin equation (GLE) approach (MFE/GLE formulation) to characterize thermal noise in confined fluids. The MFE/GLE formulation is used to compute the correlation time of the thermal noise, which is an important parameter that assigns a time scale to the thermal noise. We also use the formulation to extract the thermal force a fluid molecule experiences in a MD simulation. The remainder of the paper is organized as follows: In Sec. II, we discuss the MFE/GLE formulation. In Sec. III, we use the formulation to understand thermal noise in confined fluids. Finally, conclusions are presented in Sec. IV.

### II. MFE/GLE FORMULATION

In MFE/GLE formulation, we use the Langevin theory to characterize thermal noise in confined fluids. We assume that for confined systems in thermal equilibrium, the velocity  $v_q$  and position  $r_q$  of the fluid molecule of mass  $m$  in the direction

<sup>a)</sup>Electronic mail: [aluru@illinois.edu](mailto:aluru@illinois.edu)

$q$  at time  $t$  can be described by the GLE<sup>9-11</sup> as

$$m \frac{dv_q(t)}{dt} = -m \int_0^t K_q(t-t')v_q(t')dt' + F_q(r_q(t)) + R_q(t), \quad (1a)$$

$$\frac{dr_q(t)}{dt} = v_q(t), \quad (1b)$$

where  $K_q$  is the memory function that characterizes the velocity dependent dissipative force,  $F_q$  is the position dependent mean force that characterizes the structural inhomogeneity of the confined fluid, and  $R_q$  is an additive random force that mimics the thermal noise. Further, as  $R_q$  represents equilibrium thermal fluctuations, no instant plays a preferential role (starting sampling time is referred to as  $t = 0$ ), and we assume that it obeys the following statistical relations:

$$\langle R_q(t) \rangle = 0, \quad (2a)$$

$$\langle v_q(0)R_q(t) \rangle = 0, \quad (2b)$$

$$\langle F_q(r_q(0))R_q(t) \rangle = 0. \quad (2c)$$

Relation (2a) assumes that the mean value of the random force is zero as it does not disturb or destroy the equilibrium. Relations (2b) and (2c) assume that the thermal force is uncorrelated with the velocity and the mean force, respectively.<sup>9</sup> If we multiply Eq. (1a) by  $v_q(0)/\langle v_q(0)^2 \rangle$  and perform the ensemble averaging (angular brackets denote ensemble average) using Eq. (2b), we get,

$$\frac{d\Psi_q(t)}{dt} = - \int_0^t K_q(t-t')\Psi_q(t')dt' + \Theta_q(t), \quad (3a)$$

$$\Psi_q(t) = \langle v_q(0)v_q(t) \rangle / \langle v_q(0)^2 \rangle, \quad (3b)$$

$$\Theta_q(t) = \langle v_q(0)F_q(r_q(t)) \rangle / m \langle v_q(0)^2 \rangle, \quad (3c)$$

where  $\Psi_q(t)$  is the normalized velocity autocorrelation function ( $v$ -ACF) and  $\Theta_q(t)$  is the time-dependent cross-correlation function between the mean force and the velocity of the fluid molecule. The above integro-differential equation (Eq. (3a)) that describes the time evolution of the  $v$ -ACF of a fluid molecule inside the confined system is the MFE for a confined fluid. This equation reduces to the MFE for bulk fluids ( $F_q = 0$ ,  $\Theta_q(t) = 0$ ), which is an exact equation that can be formally derived from the Liouville equation using the projection operator formalism.<sup>10,11</sup> Thus,  $\Theta_q(t)$  can be interpreted as a measure of the additional memory that a confined fluid molecule carries because of its interaction with the confining surface. The utility of this equation is that given  $\Psi_q(t)$  and  $\Theta_q(t)$  (from experiments or MD simulations), it can be used to compute the memory function  $K_q(t)$ .

For fluids in thermal equilibrium, the fluctuation-dissipation (FD) theorem relates the memory function  $K_q(t)$  to the autocorrelation function of the random force used in the Langevin equation.<sup>11</sup> Now, we discuss that relationship. The GLE (Eq. (1a)) can be used to compute the autocorrelation

function of the random force,  $\langle R_q(0)R_q(t) \rangle$ , as

$$\begin{aligned} & \langle R_q(0)R_q(t) \rangle \\ &= m^2 \left[ \langle \dot{v}_q(0)\dot{v}_q(t) \rangle + \int_0^t K_q(t-t') \langle \dot{v}_q(0)v_q(t') \rangle dt' \right] \\ & \quad - m \langle \dot{v}_q(0)F_q(r_q(t)) \rangle, \end{aligned} \quad (4)$$

where the dot ( $\dot{\cdot}$ ) represents the derivative with respect to time. We have used the property defined in Eq. (2c) to obtain Eq. (4). Now, using the properties of the derivative of stationary autocorrelation functions,<sup>11,12</sup> and performing the algebra using Laplace transform, the above equation can be solved for  $\langle R_q(0)R_q(t) \rangle$  as

$$\langle R_q(0)R_q(t) \rangle = m^2 \langle v_q(0)^2 \rangle [K_q(t) - \Theta_q(0)\delta(t)], \quad (5)$$

where  $\delta$  is the Dirac delta function and the rest of the symbols have the same meaning as defined above. Further, using the equipartition theorem that relates the variance of the velocity to temperature  $T$  as  $\langle v_q(0)^2 \rangle = m^{-1}k_B T$  ( $k_B$  is the Boltzmann constant), and realizing that  $\Theta_q(0) = 0$  (since  $\Psi_q(t)$  is an even function in time,  $\frac{d\Psi_q}{dt}|_{t=0} = 0$  and from Eq. (3a) we get  $\Theta_q(0) = 0$ ), we can simplify the relation as

$$\langle R_q(0)R_q(t) \rangle = mk_B T K_q(t). \quad (6)$$

The utility of this relation is that the knowledge of the memory function  $K_q(t)$  that describes the  $v$ -ACF of a molecular fluidic system can provide an understanding of the autocorrelation function of the thermal noise in that system. We use this relationship to compute the correlation time of the thermal noise,  $\tau_R$ , as<sup>7</sup>

$$\tau_R \equiv \frac{\int_0^\infty |\langle R_q(0)R_q(t) \rangle| dt}{\langle R_q(0)^2 \rangle} = \frac{1}{K_q(0)} \int_0^\infty |K_q(t)| dt, \quad (7)$$

which can be compared with other characteristic time scales to understand its interplay with the underlying physical process. In this work, we compare the thermal noise correlation time with the momentum relaxation time of the fluid. Momentum relaxation time is the average time it takes for a molecule to completely randomize its state in momentum. The momentum relaxation time,  $\tau_v$ , can be estimated by using the velocity autocorrelation function in place of the thermal noise autocorrelation function in Eq. (7). Such an analysis lets one understand the interplay of thermal noise in the self-diffusion dynamics of the fluid. We now apply this approach to characterize thermal noise in molecular fluids.

### III. THERMAL NOISE IN MOLECULAR FLUIDS

We first use the MFE/GLE formulation to compute the correlation time of thermal noise in bulk fluids ( $F_q = 0$ ,  $\Theta_q(t) = 0$ ). Figures 1(a) and 1(b) show the comparison of the time decay of the center-of-mass (COM)  $v$ -ACF and the corresponding thermal noise autocorrelation function ( $R$ -ACF) for bulk carbon-dioxide ( $\text{CO}_2$ )<sup>13</sup> and extended simple point charge (SPC/E)<sup>14</sup> water, respectively. Both the  $v$ -ACF and the  $R$ -ACF are normalized by their initial values. The thermodynamic state for these fluids is reported in Table I.  $v$ -ACFs are obtained from MD simulations. MD simulation is performed

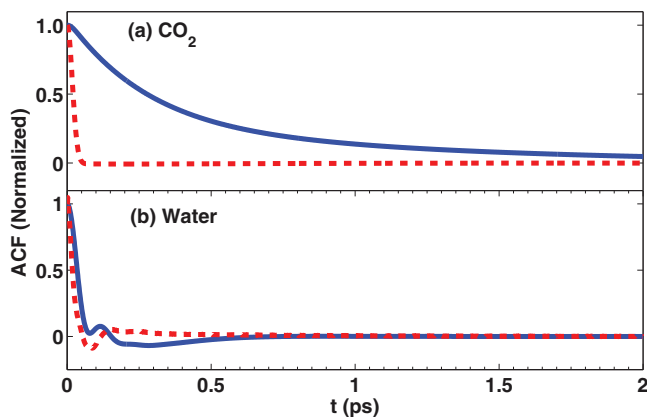


FIG. 1. Comparison of the COM  $v$ -ACF (solid line) and  $R$ -ACF (broken line) for (a) bulk  $\text{CO}_2$  and (b) bulk SPC/E water.

using the simulation package GROMACS.<sup>15</sup> Once  $v$ -ACF is known, Eq. (3a) is solved numerically to obtain  $K(t)$ , which is related to  $R$ -ACF through Eq. (6). The numerical procedure to solve Eq. (3a) is discussed in Ref. 11. It can be observed that for  $\text{CO}_2$  the  $v$ -ACF and the  $R$ -ACF are widely separated in time, while for SPC/E water they have a significant overlap. Further, the  $v$ -ACF of  $\text{CO}_2$  has an exponential type decay, which is typical of the relaxation mechanism in low density fluids where the fluid relaxes without experiencing significant backscattering from the neighboring molecules. For SPC/E water, the  $v$ -ACF shows a rapid initial decay, becomes negative because of backscattering, and then slowly decays to zero. Also, it can be observed that the  $v$ -ACF of SPC/E water has a small bump at  $t \sim 0.16$  ps before it becomes negative. It has been reported in the literature that this feature is universal to bulk water  $v$ -ACF at 1 bar pressure and 300 K temperature, and is independent of the interaction potential model used to simulate the water dynamics.<sup>16</sup> Its origin can be related to the rotational induced translation due to a combined effect of Lennard-Jones (LJ) and Coulomb interactions.

We use the  $v$ -ACFs and  $R$ -ACFs to compute the noise correlation time ( $\tau_R$ ) and the momentum relaxation time ( $\tau_v$ ) for these fluids. The correlation times are computed using Eq. (7) and are reported in Table I. It can be observed that for  $\text{CO}_2$  the correlation time of thermal noise is about an order of magnitude smaller than the momentum relaxation time ( $\tau_v/\tau_R \sim 15$ ), while for bulk water the noise and the momentum relaxation times are of the same order ( $\tau_v/\tau_R \sim 1$ ). It is only when the thermal noise correlation time is much smaller than the characteristic time scale of the system, it can be

TABLE I. Thermal noise correlation time,  $\tau_R$ , and the momentum relaxation time,  $\tau_v$ , in fluidic systems.

System	$\rho$ ( $\#/\text{nm}^3$ )	$T$ (K)	$\tau_R$ (ps)	$\tau_v$ (ps)
Bulk $\text{CO}_2$	9	323	0.03	0.51
Bulk SPC/E water	33.3	300	0.06	0.06
SPC/E water (6,6) CNT <sup>a</sup>	...	300	0.35	0.22
SPC/E water (16,16) CNT <sup>a</sup>	...	300	0.05	0.06
SPC/E water (30,30) CNT <sup>a</sup>	...	300	0.06	0.06

<sup>a</sup>CNT is loaded at 1 bar pressure and 300 K temperature.

assumed uncorrelated with the underlying physical process and “White” noise description is valid. When the two time scales are of comparable order, the memory effects become important and the finite correlation time of the thermal noise must be taken into account to understand the interplay of thermal noise. Our conclusion for bulk water is consistent with the results of Liu, Harder, and Berne,<sup>17</sup> where they show the inability of the Gaussian White-noise in capturing the short-time self-diffusion dynamics of TIP4P water molecules in the bulk state. Also, we want to point out that the noise correlation time for bulk SPC/E water computed here ( $\tau_R \sim 0.06$  ps) is lower than the value of  $\sim 2$  ps reported in Ref. 18. The reason for this discrepancy is that in Ref. 18 the autocorrelation function of the force that the oxygen atom of the water molecule experiences in a MD simulation is used to compute the correlation time of thermal noise.

We now use the MFE/GLE formulation to study thermal noise in confined fluids. For fluids confined inside nanometer scale geometries, due to the strong interaction of the fluid molecules with the confining wall, the fluid becomes inhomogeneous and its static and dynamical properties are different in the direction parallel and perpendicular to the confining surface.<sup>19</sup> We study the properties of thermal noise in both the directions. The first system we study is SPC/E water confined inside a  $11\sigma_{oo}$  wide ( $\sigma_{oo}$  is the LJ interaction distance parameter of the oxygen atom of SPC/E water molecule;  $\sigma_{oo} = 0.317$  nm<sup>14</sup>) semi-infinite graphite slit pore. The system is loaded at a reference bulk state of 33.3 molecules/nm<sup>3</sup> and 300 K temperature. Figure 2(a) shows a schematic diagram of the semi-infinite slit pore system (slit is infinite in  $x$  and  $y$  directions and  $z$  is the confining direction). The molecular modeling and MD simulation details for all the confined systems considered in this work can be found in Refs. 20 and 21. Figure 2(b) shows the variation of the local number density  $\rho(z)$  of the water molecules across the confinement. To understand the effect of confinement, we divide the slit into three regions, Reg. I, II, and III, based on their perpendicular distance from the confining wall. Figures 2(c) and 2(d) show the variation of the mean force,  $F_q$ , in the three regions along the perpendicular ( $q = z$ ) and the parallel ( $q = x$ ) directions, respectively. It can be observed that  $F_z$  is oscillatory in Regs. I and II, and is a constant  $\sim 0$  in Reg. III, thus giving rise to an inhomogeneous density profile near the confining surface and a bulk-like homogeneous density in the central region of the pore. The variation of  $F_x$  is very small ( $\sim 0$ ) in all the three regions, which suggests that the lattice structure of the graphite wall does not induce structural inhomogeneity along the parallel direction. Figure 2(e) shows the comparison of the COM  $v$ -ACF of water along  $x$  (broken line) and  $z$  (solid line) directions in the three regions. The  $v$ -ACFs are normalized by their initial value. It can be observed that in Reg. I, which is nearest to the wall, the time decay of the  $v$ -ACF in  $x$  and  $z$  directions is significantly different from each other, confirming that the dynamical behavior of the fluid molecules is highly anisotropic. In Regs. II and III, the  $v$ -ACFs in both directions look quite similar to each other. It is interesting to observe that in Reg. II, though the density profile is quite inhomogeneous (see Fig. 2(b)), the two  $v$ -ACFs are not significantly different from each other. With  $v$ -ACFs known from

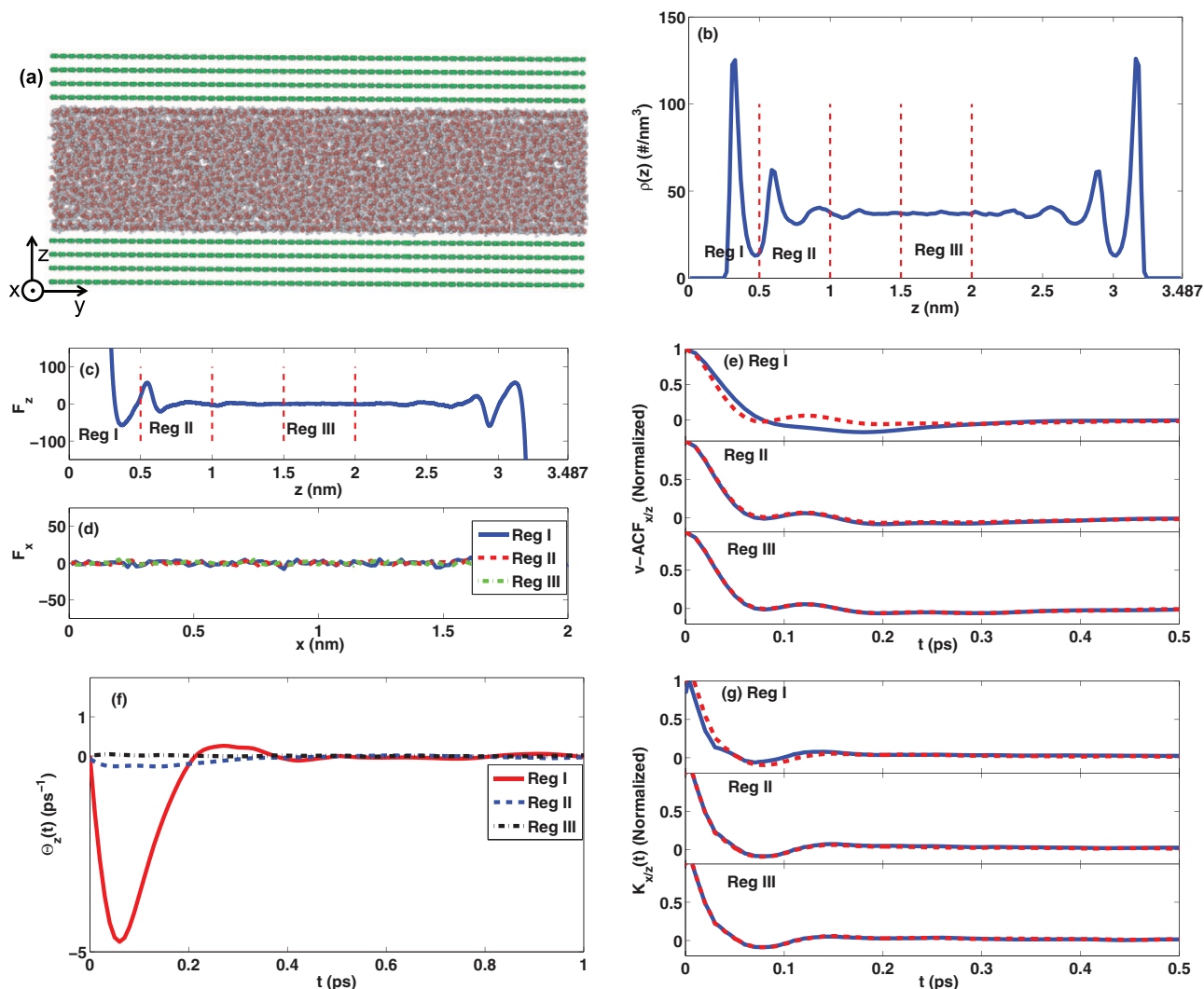


FIG. 2. (a) Schematic of a semi-infinite slit pore, (b) number density  $\rho(z)$ , (c) and (d) mean force profiles (force is in kJ/mol-nm), (e)  $v$ -ACFs along  $x$  (broken line) and  $z$  (solid line) directions, (f) variation of  $\Theta_z(t)$ , and (g) memory functions  $K_{xz}(t)$  (broken line) and  $K_{zz}(t)$  (solid line) of SPC/E water confined inside a graphite slit.

MD simulation, we now use the MFE to compute the memory function in each region. It can be observed from Eq. (3a) that for confined fluids the time evolution of  $v$ -ACF is governed by a combined effect of the dynamical response due to the interaction of the fluid molecules with the confining surface ( $\Theta_q(t)$ ) and the thermal noise ( $K_q(t)$ ). To solve Eq. (3a) for  $K_q(t)$ , we also need to compute the function  $\Theta_q(t)$  in each region. To compute  $\Theta_q(t)$ , we need the positions  $r_q$  (to compute the mean force  $F_q$ ) and the velocity  $v_q$ , both of which are directly obtained from MD simulation. Since  $F_x$  is  $\sim 0$ , in all the three regions, the cross-correlation function  $\Theta_x(t)$  is also negligible in all the three regions. Figure 2(f) shows the variation of the function  $\Theta_z(t)$  in the three regions. It can be observed that  $\Theta_z(t)$  provides a significant short time contribution (until 0.5 ps) in Reg. I, while it is almost zero in Regs. II and III. We use  $\Theta_q(t)$  and  $v$ -ACF of each region and direction (total 6 cases) in Eq. (3a) and numerically compute  $K_q(t)$ . Figure 2(g) shows the comparison of the memory functions,  $K_{xz}(t)$ , along  $x$  (broken line) and  $z$  (solid line) directions in the three regions. Similar to  $v$ -ACFs, the memory functions are also normalized by their initial value ( $K_{xz}(0)$ ). It can be

observed that the time decay of the memory functions along  $x$  and  $z$  directions in each region is quite similar to each other. Also, the time decay of the memory functions in the three regions do not differ significantly from each other. The correlation time of the thermal noise (computed using Eq. (7)) in the three regions along both the directions is found to be quite similar and is  $\sim [0.05-0.06]$  ps. These observations suggest that even though the dynamical behavior of the confined fluid is spatially anisotropic, the correlation time and the time decay of the thermal noise autocorrelation function are not significantly different across the confinement. Further, from Eq. (3a) we can deduce that it is the strong cross-correlation of the mean force with the molecular velocity (characterized by the function  $\Theta_q(t)$ ) that gives rise to the spatial anisotropy in the  $v$ -ACF of the confined fluid.

To investigate further on the statistical properties of the thermal noise in each region, we use the computed memory functions in the GLE and extract the thermal force from the total force that a particle experiences in a MD simulation. If  $F_q^{tot}(t)$  is the total instantaneous force at time  $t$  along the direction  $q$ , then Eq. (1a) can be written for

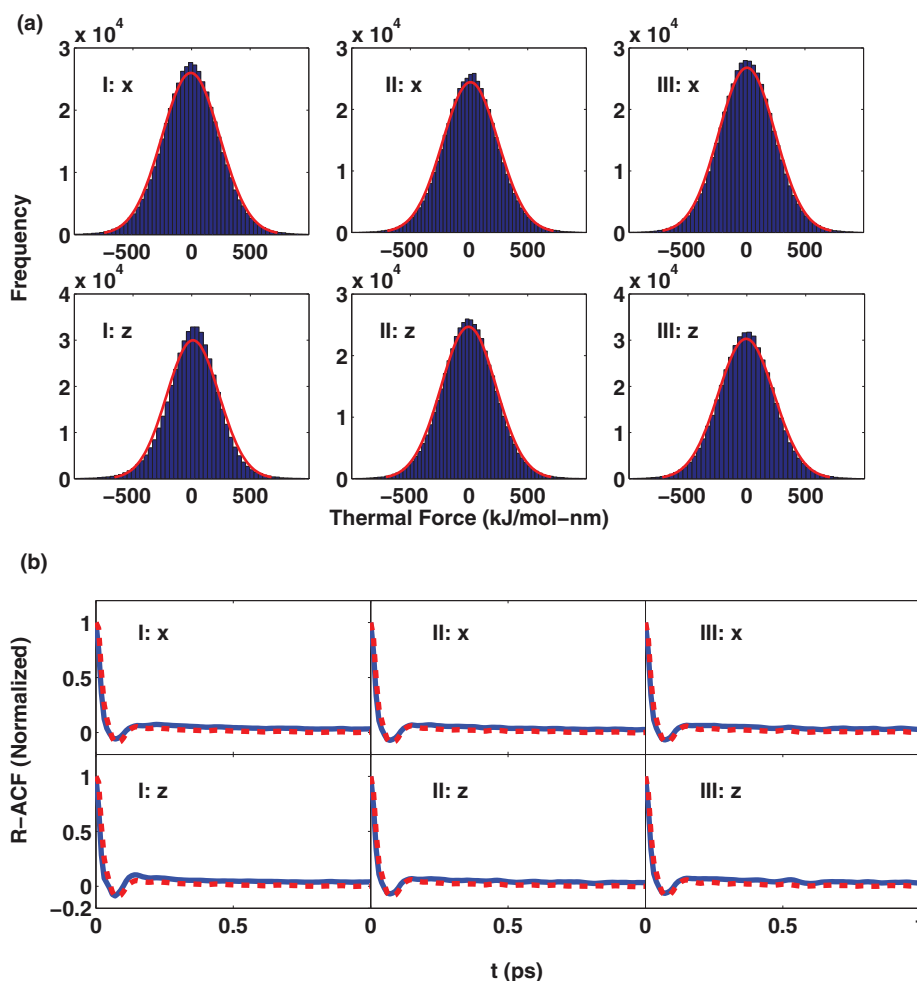


FIG. 3. (a) Frequency distribution of the thermal force, (b) verification of the FD relation (solid line is the normalized  $R$ -ACF obtained from MD and broken line is  $K_q(t)/K_q(0)$ ) in different regions for SPC/E water confined inside a graphite slit.

$R_q(t)$  as

$$R_q(t) = [F_q^{tot}(t) - F_q(r_q(t))] + m \int_0^t K_q(t-t')v_q(t')dt'. \quad (8)$$

The total force, velocity, and position at each instant can be directly obtained from MD simulation and the above equation can be solved numerically to obtain  $R_q(t)$ . To minimize the artificial effects of MD thermostats, MD simulation was performed in the NVE ensemble, where  $N$  is the number of particles,  $V$  is the volume, and  $E$  is the total energy of the system. We extract the thermal force and estimate the frequency

distribution of the thermal force for each region and direction. Figure 3(a) shows the comparison of the frequency distribution of the thermal force along  $x$  and  $z$  directions for each region. Table II shows the mean, variance, skewness, and Kurtosis value of the thermal force extracted from the MD simulation. It can be observed that the distribution function of the thermal force in all three regions qualitatively resemble a zero mean Gaussian distribution, which is typically assumed to model thermal noise in molecular fluids. It can be observed from Table II that the mean of the thermal force is  $\sim 0$  for all regions and directions. Also, for Reg. I, which is nearest to the confining surface, the variance of the thermal force

TABLE II. Statistical moments of the thermal force  $R_q(t)$  for confined water<sup>a</sup> as extracted from the MD simulation.

Reg.	Direction	Mean	Variance	Skewness	Kurtosis	$K_q(0)$	$mk_BTK_q(0)$
I	$x$	$-3.7 \pm 52.3$	$5.71 \times 10^4 \pm 4.9 \times 10^3$	$-0.012 \pm 0.08$	$3.65 \pm 0.22$	1211	$5.44 \times 10^{+4}$
I	$z$	$11.2 \pm 36.8$	$4.85 \times 10^4 \pm 6.9 \times 10^3$	$-0.29 \pm 0.20$	$4.29 \pm 0.47$	1123	$5.04 \times 10^{+4}$
II	$x$	$1.01 \pm 47.3$	$5.39 \times 10^4 \pm 2.8 \times 10^3$	$0.004 \pm 0.07$	$3.65 \pm 0.23$	1231	$5.53 \times 10^{+4}$
II	$z$	$-3.37 \pm 51.4$	$5.23 \times 10^4 \pm 4.2 \times 10^3$	$-0.034 \pm 0.10$	$3.66 \pm 0.24$	1261	$5.66 \times 10^{+4}$
III	$x$	$1.74 \pm 45.9$	$5.42 \times 10^4 \pm 2.5 \times 10^3$	$0.002 \pm 0.08$	$3.62 \pm 0.24$	1233	$5.54 \times 10^{+4}$
III	$z$	$-1.97 \pm 45.2$	$5.41 \times 10^4 \pm 2.7 \times 10^3$	$0.004 \pm 0.08$	$3.63 \pm 0.22$	1240	$5.57 \times 10^{+4}$

<sup>a</sup>System: SPC/E water confined inside a  $11\sigma_{oo}$ -wide graphite slit pore.

along the  $z$  direction is lower than that of the  $x$  direction. For Regs. II and III, the variance along  $x$  and  $z$  directions are quite similar to each other. Further, it is interesting to note that for all regions and directions, the skewness value (third moment) is not strictly zero and the Kurtosis value (fourth moment) is greater than 3. A non-zero skewness value and a Kurtosis value greater than 3 suggest that thermal noise is not strictly Gaussian. We also report in Table II the initial value of the memory function  $K_q(0)$  and the theoretical variance value ( $\langle R_q(0)^2 \rangle = mk_B TK_q(0)$ ) for each region and direction. It can be observed that within statistical uncertainty, the variance of the thermal force extracted from the MD simulation for all directions and regions is in agreement with their respective theoretical values. Thus, the noise extraction from MD simulation suggests that frequency distribution of the thermal force is non-Gaussian and its distribution near the confining surface is different in the direction parallel and perpendicular to the confinement. We also used the extracted thermal force to verify the FD relation for this system. Figure 3(b) shows the verification of the FD relation along each direction in the three regions. The solid line is the normalized  $R$ -ACF ( $\langle R_q(0)R_q(t) \rangle / \langle R_q(0)^2 \rangle$ ) computed using the  $R_q(t)$  values extracted from the MD simulation and broken line is the ratio  $K_q(t)/K_q(0)$ . The verification of the FD relation confirms the physical validity of the MFE/GLE approach to extract thermal

noise in molecular fluids. We also repeated our calculations by performing a MD simulation for this system using the simulation package LAMMPS.<sup>24</sup> The aim was to ensure that the MD inputs to the MFE/GLE formulation are the same from both LAMMPS and GROMACS. The  $v$ -ACFs, cross-correlation functions  $\Theta_q(t)$ , and memory functions  $K_q(t)$  obtained from LAMMPS were found to be almost identical to those obtained from GROMACS. To check if the non-Gaussian features observed in the confined fluid are also observed in the bulk fluid, we extracted and analyzed thermal noise in the bulk SPC/E water at the same thermodynamic state. For bulk water too the Kurtosis value was found greater than 3. It has been reported in the literature that non-Gaussian behavior is also observed in the velocity autocorrelation function of dense bulk fluids.<sup>22,23</sup>

To show the generality of these observations to a different confining surface, we use the formulation to study thermal noise for SPC/E water confined inside a  $4\sigma_{oo}$  wide semi-infinite silicon slit pore. This system is also loaded at a reference bulk state of 33.3 molecules/nm<sup>3</sup> and 300 K temperature.<sup>20</sup> Figure 4(a) shows the variation of the local density  $\rho(z)$  across the confinement. It can be observed that for this system the density profile of water is completely inhomogeneous across the confinement. Here again we divide the slit into two regions (Reg. I and II) to understand the effect of the confinement. Figures 4(b) and 4(c) show the variation of

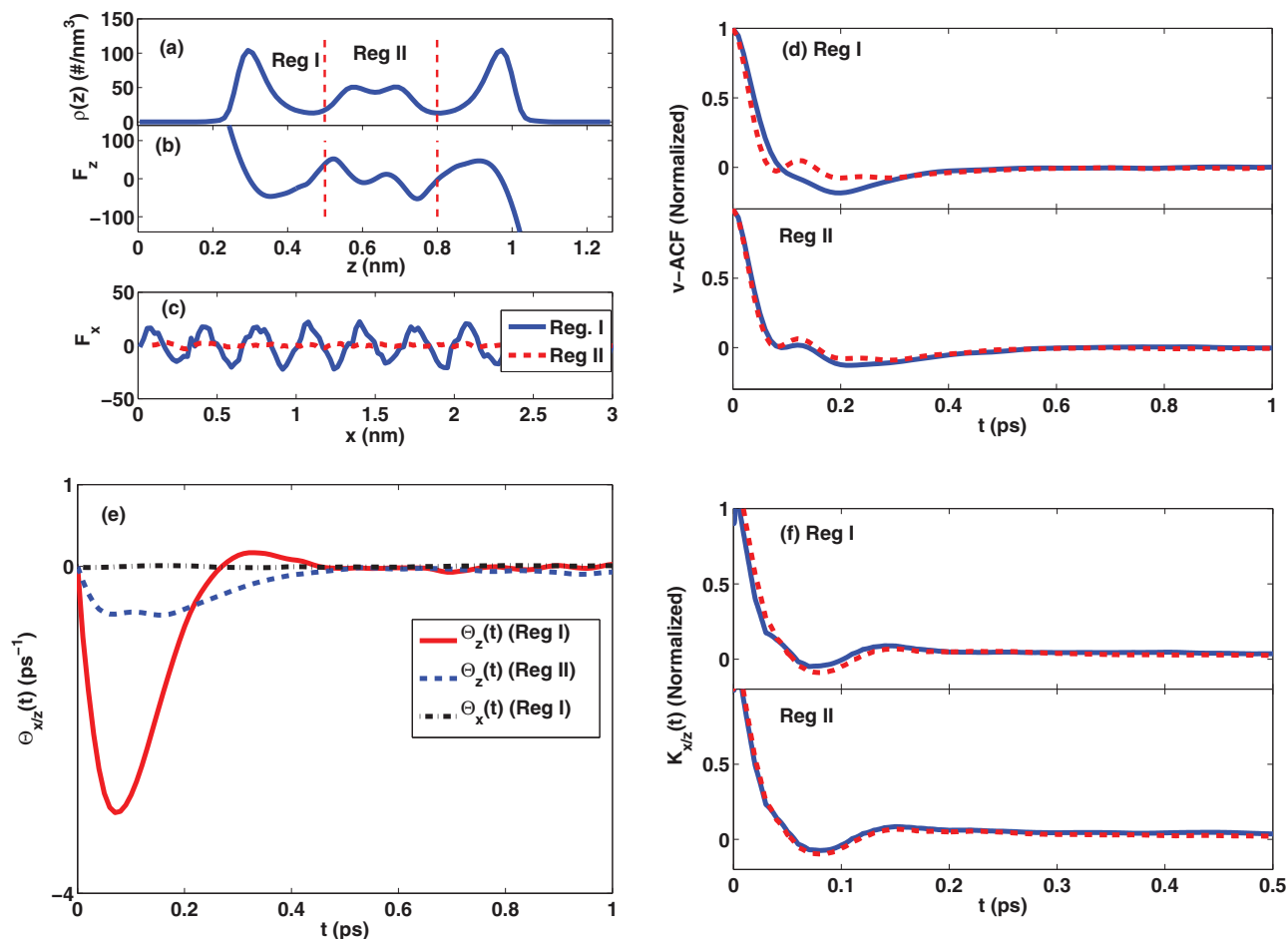


FIG. 4. (a) Number density  $\rho(z)$ , (b) and (c) mean force profiles (force is in kJ/mol-nm), (d)  $v$ -ACFs along  $x$  (broken line) and  $z$  (solid line) directions, (e) variation of  $\Theta_z(t)$ ,  $\Theta_x(t)$ , and (f) memory functions  $K_x(t)$  (broken line) and  $K_z(t)$  (solid line) of SPC/E water confined inside a silicon slit.

the mean force along  $z$  and  $x$  directions, respectively. It can be observed that for this system,  $F_x$  varies periodically in Reg. I. This periodic variation of  $F_x$  characterizes the effect of the lattice structure of the silicon wall and gives rise to structural inhomogeneity along the parallel direction. Figures 4(d)–4(f) show the COM  $v$ -ACFs, cross-correlation functions  $\Theta_{x/z}(t)$ , and memory functions  $K_{x/z}(t)$ , respectively, for this system. It can be observed that even for this system the time decay of the memory functions (Fig. 4(f)) in the two regions along both directions is quite similar to each other. For this system too, it is the strong cross-correlation of the mean force with the molecular velocity that gives rise to the dynamical anisotropy in the  $v$ -ACF near the confining surface. It is interesting to note that though the magnitude of  $F_x$  oscillates with a finite non-zero magnitude in Reg. I, function  $\Theta_x(t)$  (Fig. 4(e)) is quite small in comparison to  $\Theta_z(t)$ . This is because the magnitude of  $F_x$  is much smaller than that of  $F_z$ . We also performed this study for SPC/E water confined inside different size graphene slit pores, and for CO<sub>2</sub> and LJ argon confined inside different size graphite slit pores. The physical findings obtained for these systems were also found to be consistent with the findings reported above.

Now, we use the MFE/GLE approach to compute the correlation time of thermal noise for water confined inside a (6,6) CNT. The motivation of this study is to understand if the preferential orientation of the hydrogen bond of water molecules inside a (6,6) CNT can affect the correlation time of thermal noise. In the bulk state, water forms on an average 4 hydrogen bonds, but the molecules are pulled or pushed by their hydrogen bonds isotropically without any preferential direction. Inside smaller size CNTs, specifically (6,6) CNT, the average number of hydrogen bonds that a water molecule forms is between 1 and 2 but they act mainly along the axis of the CNT and present a very strong correlation between the neighboring water molecules.<sup>25</sup> Because of these highly coordinated hydrogen bonds, water forms a twisted spiral-like single-file chain where two water molecules cannot cross each other.<sup>26</sup> Though water forms a single-file chain, it has been reported in several MD simulation studies that the diffusion mechanism of water inside (6,6) CNT exhibits an initial ballistic motion, which, in the long run, changes to Fickian.<sup>27</sup> As long as the mean-square-displacement (MSD) exhibits a Fickian dynamics at long times, the GLE (Eq. (1a)) can be used to model the stochastic dynamics of water inside a (6,6) CNT.<sup>28</sup> We apply the MFE/GLE approach to compute the noise correlation time for SPC/E water confined inside (6,6), (16,16), and (30,30) CNTs, which are loaded at the same thermodynamic state. The CNTs are infinitely long and are loaded at 1 bar pressure and 300 K temperature. The molecular modeling and MD simulation details for water-CNT systems can be found in Ref. 29. Figures 5(a) and 5(b) show the comparison of the COM  $v$ -ACFs and the corresponding memory functions  $K(t)$ , respectively, of the water molecules along the axial direction for each CNT. Also, for comparison, we plot the  $v$ -ACF and the memory function of bulk water at 1 bar pressure and 300 K temperature. Both the  $v$ -ACF and the memory function are normalized by their initial value. It can be observed that the time decay of both the  $v$ -ACFs and the memory functions of the water molecules inside (30,30) and (16,16) CNTs (see

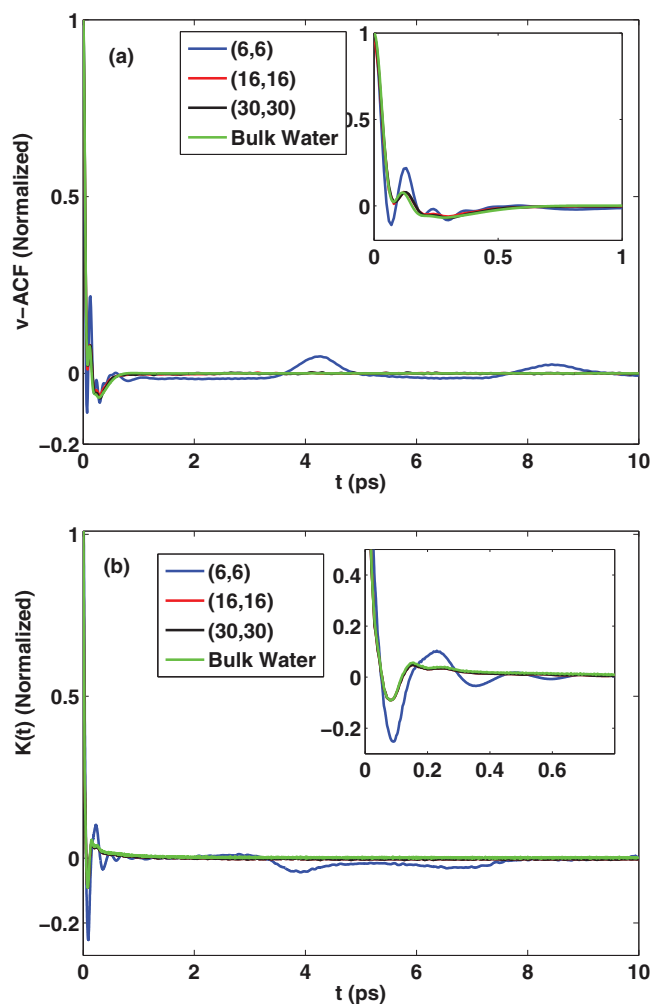


FIG. 5. (a)  $v$ -ACF (Inset: Enlarged view [0-1] ps) and (b) memory function  $K(t)$  (Inset: Enlarged view [0-0.8] ps) of SPC/E water confined inside different-size CNTs.

insets) are very similar to that of bulk water. For (6,6) CNT, it can be observed that both the short time (see insets) and the long-time behavior of the  $v$ -ACF and the memory function are significantly different from that of bulk water. The  $v$ -ACF shows a distinctive hump starting at  $\sim 4$  ps, which re-occurs at  $\sim 8$  ps, albeit with a smaller magnitude before eventually decaying to zero. We have time averaged the  $v$ -ACF up to 6 ns to ensure that these humps are not statistical noise. These long time non-zero correlations, which are absent in the bulk state and bigger size CNTs are the characteristics of the highly concerted single-file motion of the water molecules inside a (6,6) CNT. We use the computed memory functions to estimate the noise correlation time for these systems. The thermal noise correlation times are reported in Table I. Also, for comparison, we report the momentum relaxation time of water in these systems. It can be observed from Table I that for (6,6) CNT, the noise correlation time is  $\sim 0.35$  ps, which is around 5 times bigger than that of bulk water (0.06 ps). For (16,16) and (30,30) CNT, the noise correlation time is same as that of bulk water. Also, it can be observed from Table I that the ratio of the noise and momentum relaxation times in these systems is  $\sim 1$ , suggesting that thermal noise cannot be

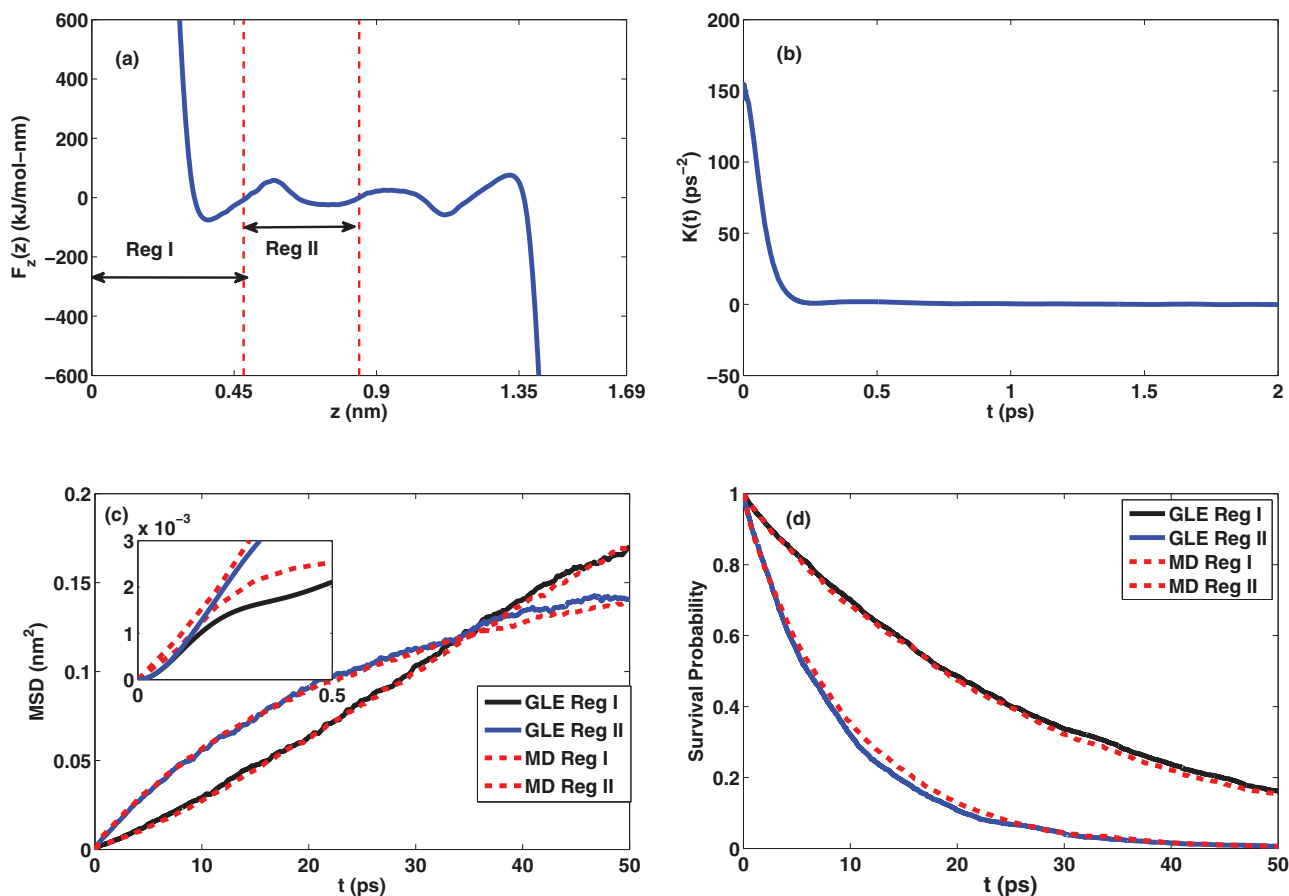


FIG. 6. (a) Mean force profile  $F_z$ , (b) memory function  $K(t)$ , (c) MSD (Inset: Enlarged view [0-0.5] ps), and (d) survival probability of confined LJ argon as obtained from GLE and MD simulations.

assumed uncorrelated and its finite correlation time must be accounted for to understand the interplay of thermal noise in these systems.

Now, we discuss an example which demonstrates that assuming the thermal noise to be spatially isotropic and Gaussian distributed does reproduce important single-particle dynamical properties of confined fluids. Though our study reveals that thermal force is not strictly Gaussian distributed, we still assume it to be Gaussian. The reason for assuming the noise to be Gaussian is purely a mathematical simplicity as a correlated Gaussian distribution can be easily generated numerically. Further, such an exercise will let us understand what sort of discrepancies can occur in the computed quantities if the non-Gaussian features are ignored in modeling thermal noise. The system we choose is a high density LJ argon (Ar) (average density  $18.5 \text{ atoms/nm}^3$  and temperature 300 K) confined inside a  $5\sigma_{ArAr}$  wide ( $\sigma_{ArAr}$  is LJ interaction distance parameter;  $\sigma_{ArAr} = 0.34 \text{ nm}$ <sup>30</sup>) semi-infinite graphite slit. The reason for choosing this system is that in one of our earlier studies<sup>31</sup> this system showed maximum quantitative difference in the computed single-particle quantities when the finite correlation time of thermal noise was ignored and thermal fluctuations were modeled as Gaussian White noise. Figures 6(a) and 6(b) show the mean force profile  $F_z$  and the memory function  $K(t)$ , respectively, for this system. The mean force profile  $F_z$  is obtained from an empirical potential based quasi-continuum theory (EQT).<sup>30,32</sup> Memory function  $K(t)$  is

obtained by using the MFE/GLE formulation and we take the memory function of Reg. II (see Fig. 6(a)) to be the representative memory function for the entire system. The thermal noise correlation time of LJ Ar in this system can be estimated using Eq. (7) and is  $\sim 0.08$  ps. With the mean force profile and the memory function known, we solve Eqs. (1a) and (1b) to compute the position and velocity of the confined fluid molecule in the perpendicular ( $q = z$ ) direction. We use an approximate frequency domain method to generate correlated Gaussian random numbers  $R_z(t)$ . The algorithm is discussed in Ref. 33. A stochastic version of the Verlet algorithm is used to numerically integrate the GLE in time. This integration scheme is discussed in Ref. 34. The simulation is used to compute the MSD and survival probability of argon in different regions across the confinement (see Fig. 6(a)). In confined fluids, the position dependent MSD,  $\langle [r_q(t) - r_q(t_0)]^2 \rangle$ , along the direction  $q$  can be computed as<sup>31</sup>

$$\langle [r_q(t) - r_q(t_0)]^2 \rangle = \frac{1}{J} \sum_{j=1}^J \frac{1}{N_j(t_0)} \sum_{i=1}^{N_j(t_0)} [r_q^i(t) - r_q^i(t_0)]^2, \quad (9)$$

where  $r_q^i(t_0)$  is the position of a molecule  $i$  at the starting time  $t_0$ ,  $r_q^i(t)$  is its position at a later time  $t$  and  $N_j(t_0)$  is the number of particles present in the region of interest at the starting time  $t_0$ . In this sampling scheme, a particle is assigned to a particular region if it was present in that region at the starting

time  $t_0$ . The simulation time is partitioned into blocks and the sampling process is repeated  $J$  times to perform block averaging. Survival probability is defined as the average probability that a particle which was inside a region at time  $t_0$  still remains inside that region at a later time  $t$ . For a region,  $q_L \leq q \leq q_U$ , the survival probability,  $P([q_L, q_U], t; [q_L, q_U], t_0)$ , is computed as<sup>17,31</sup>

$$P([q_L, q_U], t; [q_L, q_U], t_0) = \frac{1}{J} \sum_{j=1}^J \frac{N_j(t)}{N_j(t_0)}, \quad (10)$$

where  $N_j(t_0)$  is the number of particles present in the region at time  $t_0$ , and  $N_j(t)$  is the number of those particles which still remain in the region after time  $t - t_0$ . Survival probability is a boundary dependent quantity and its accuracy is quite sensitive to the resolution of the short time dynamics.<sup>17</sup> Figures 6(c) and 6(d) show the comparison of the MSD and survival probability, respectively, in different regions as obtained from GLE and MD simulations. It can be observed that the results obtained by assuming the thermal noise to be isotropic and Gaussian distributed are in reasonably good agreement with those obtained from MD simulation. What quantities and what length and time scale can get effected by ignoring the non-Gaussian features of thermal noise is under investigation.

#### IV. CONCLUSIONS

In this work, we discuss a combined MFE/GLE formulation to characterize thermal noise in confined fluids. Our study reveals that the correlation time and the time decay of the autocorrelation function of the thermal noise are not significantly different across the confinement. We show that it is the cross-correlation of the mean force with the molecular velocity that gives rise to the spatial anisotropy in the velocity-autocorrelation function of the confined fluids. Further, we used the MFE/GLE formulation to extract the thermal force that a single particle experiences in MD simulations. Noise extraction from MD simulation revealed that for both bulk and confined fluids the distribution function of the thermal force is not strictly Gaussian. Also, the frequency distribution of the thermal force near the confining surface is found to be different in the direction parallel and perpendicular to the confinement. We also used the formulation to compute the noise correlation time for water confined inside different size CNTs. It is found that inside the (6,6) CNT, in which water arranges itself in a highly concerted single-file arrangement, the correlation time of thermal noise is an order of magnitude larger than that of bulk water. We also discuss an example which demonstrates that assuming the thermal noise to be spatially isotropic and Gaussian distributed in the GLE can be used

to simulate important single-particle dynamical properties of confined fluids.

#### ACKNOWLEDGMENTS

This work was supported by the AFOSR under Grant No. FA9559-12-1-0464 and by NSF under Grant No. 1264282. T.S. wishes to thank R. Bhaduria for helping with LAMMPS simulations. The authors acknowledge the use of the Taub cluster provided by the Computational Science and Engineering Program at the University of Illinois.

- <sup>1</sup>R. Fetzer, M. Rauscher, R. Seemann, K. Jacobs, and K. Mecke, *Phys. Rev. Lett.* **99**, 114503 (2007).
- <sup>2</sup>L. Bocquet and E. Charlaix, *Chem. Soc. Rev.* **39**, 1073 (2010).
- <sup>3</sup>A. Kalra, S. Garde, and G. Hummer, *Proc. Natl. Acad. Sci. U.S.A.* **100**, 10175 (2003).
- <sup>4</sup>R. Wan, J. Hu, and H. Fang, *Sci. China: Phys., Mech. Astron.* **55**, 751 (2012).
- <sup>5</sup>F. Detcheverry and L. Bocquet, *Phys. Rev. Lett.* **109**, 024501 (2012).
- <sup>6</sup>F. Detcheverry and L. Bocquet, *Phys. Rev. E* **88**, 012106 (2013).
- <sup>7</sup>P. Hanggi and P. Jung, *Advances in Chemical Physics* (John Wiley and Sons, Inc., 1995), Vol. **89**.
- <sup>8</sup>J. T. Padding and A. A. Louis, *Phys. Rev. E* **74**, 031402 (2006).
- <sup>9</sup>R. Kubo, *Rep. Prog. Phys.* **29**, 255 (1966).
- <sup>10</sup>J. P. Boon and S. Yip, *Molecular Hydrodynamics* (McGraw-Hill Inc., 1980).
- <sup>11</sup>B. J. Berne and G. D. Harp, *Advances in Chemical Physics* (John Wiley and Sons, Inc., 1970), Vol. **17**, pp. 102–106, 217–222.
- <sup>12</sup>J. S. Bendat and A. G. Piersol, *Random Data: Analysis and Measurement Procedures*, 4th ed. (John Wiley and Sons, Inc., 2010), pp. 109–171.
- <sup>13</sup>Z. Zhang and Z. Duan, *J. Chem. Phys.* **122**, 214507 (2005).
- <sup>14</sup>H. Berendsen, J. Grigera, and T. Straatsma, *J. Phys. Chem.* **91**, 6269 (1987).
- <sup>15</sup>E. Lindahl, B. Hess, and D. van der Spoel, *J. Mol. Mod.* **7**, 306 (2001).
- <sup>16</sup>U. Balucani, J. P. Brodholt, and R. Vallauri, *J. Phys.: Condens. Matter* **8**, 6139 (1996).
- <sup>17</sup>P. Liu, E. Harder, and B. J. Berne, *J. Phys. Chem. B* **108**, 6595 (2004).
- <sup>18</sup>Z. Zhu, N. Sheng, R. Wan, and H. Fang, "Intrinsic autocorrelation time of picoseconds for thermal noise in water," *J. Phys. Chem. A* **118**(39), 8936–8941 (2014).
- <sup>19</sup>G. E. Karniadakis, A. Beskok, and N. R. Aluru, *Microflows and Nanoflows: Fundamentals and Simulation* (Springer Science+Business Media, Inc., New York, 2005), pp. 375–381.
- <sup>20</sup>S. Mashayak and N. R. Aluru, *J. Chem. Theory Comput.* **8**, 1828 (2012).
- <sup>21</sup>S. Mashayak and N. R. Aluru, *J. Chem. Phys.* **137**, 214707 (2012).
- <sup>22</sup>U. Balucani, V. Tognetti, R. Vallauri, P. Grigolini, and P. Marin, *ZPhys-e-B: Condens. Matter* **49**, 181 (1982).
- <sup>23</sup>G. Sese, E. Guardia, and J. A. Padro, *J. Stat. Phys.* **60**, 501 (1990).
- <sup>24</sup>S. Plimpton, *J. Comput. Phys.* **117**, 1 (1995).
- <sup>25</sup>J. C. Rasaiah, S. Garde, and G. Hummer, *Annu. Rev. Phys. Chem.* **59**, 713 (2008).
- <sup>26</sup>S. Joseph and N. Aluru, *Phys. Rev. Lett.* **101**, 064502 (2008).
- <sup>27</sup>A. Alexiadis and S. Kassinos, *Chem. Rev.* **108**, 5014 (2008).
- <sup>28</sup>S. Kou, *Ann. Appl. Stat.* **2**, 501 (2008).
- <sup>29</sup>A. B. Farimani and N. R. Aluru, *J. Phys. Chem. B* **115**, 12145 (2011).
- <sup>30</sup>T. Sanghi and N. R. Aluru, *J. Chem. Phys.* **132**, 044703 (2010).
- <sup>31</sup>T. Sanghi and N. R. Aluru, *J. Chem. Phys.* **138**, 124109 (2013).
- <sup>32</sup>A. V. Raghunathan, J. H. Park, and N. R. Aluru, *J. Chem. Phys.* **127**, 174701 (2007).
- <sup>33</sup>D. B. Percival, *Comput. Sci. Stat.* **24**, 534 (1992).
- <sup>34</sup>M. Berkowitz, J. Morgan, and J. A. McCammon, *J. Chem. Phys.* **78**, 3256 (1983).